MICROMECHANICAL MODEL FOR 3D GENERALLY ORTHOTROPIC GRID-REINFORCED COMPOSITES

E M Hassan[a], A L Kalamkarov[a], A V Georgiades[b]

[a] Department of Mechanical Engineering , Dalhousie University, Halifax, Nova Scotia, B3J 2X4, Canada

[b] Department of Mechanical Engineering and Materials Science and Engineering, Cyprus University of Technology, Limassol, Cyprus

E-mail: edris@dal.ca

SUMMARY

A micromechanical model for 3D composites with an embedded periodic grid of generally orthotropic reinforcements is developed and applied to anisotropic structures with cubic, conical and diagonal reinforcement orientations to calculate effective elastic coefficients. The model allows flexibility in the design of such structures with desirable coefficients by changing material and/or geometric parameters.

Keywords: *Asymptotic Homogenization; Grid-Reinforced Composite Structures; Orthotropic reinforcement; Effective Elastic Coefficients*.

INTRODUCTION

Recent years have witnessed a considerable increase in the use composite materials in various engineering applications such as aerospace, automotive, and marine engineering, medical prosthetic devices, sports, and recreational goods. Large-scale introduction of composite materials into novel applications can be significantly facilitated if their macroscopic behavior can be predicted at the design stage. Accordingly, comprehensive micromechanical models must be developed. To obtain more effective micromechanical models it is common practice to analyze composite materials using two scales, microscopic and macroscopic. The former recognizes the behavior and individual characteristics of the various constituents while the later amounts to dealing with the global behavior of composite material structure as an individual entity. The presence of the microscopic and macroscopic scales in the original problem frequently renders the pertinent partial differential equations extremely difficult to solve. To simplify the analysis the two scales are decoupled and each one handled independently; one technique that permits us to accomplish this is the asymptotic homogenization method. The mathematical structure of asymptotic homogenization can be found in Bensoussan et al [1]. Modeling of composites made up of inclusions embedded in a matrix has been the focus of interest of many researchers in the past half-century. In particular, the asymptotic homogenization method has been used to study periodic composite and smart structures, see e.g., Duvaut [2] and Caillerie [3]. A wide range of elasticity and thermoelasticity problems are examined by Kalamkarov [4] and the effective piezoelastic coefficients of the homogenized structure are

calculated by Kalamkarov and Kolpakov [5]. Kalamkarov and Georgiades [6, 7] derived expressions for the effective elastic, piezoelectric, and hygrothermal expansion coefficients for 3D periodic smart structures. Later on, a 3D micromechanical model is developed and applied to thin smart composite plates reinforced with a network of cylindrical reinforcements that may exhibit piezoelectric behaviour; see Georgiades et al [8]. Challagulla et al [9] developed a comprehensive 3D asymptotic homogenization model pertaining to periodic composite structures with isotropic reinforcements.

This paper proposes a novel micromechanical model for 3D generally orthotropic grid-reinforced periodic composites, see Fig. 1.

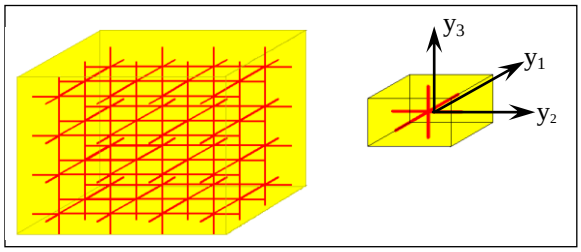

Fig. 1: 3D Grid Reinforced Composite Structure

ASYMPTPIC HOMOGENIZATION MODEL FOR 3D COMPOSITES

General Model

The problem is represented by a periodic structure obtained by repeating a small *unit cell Y* in a composite representing an inhomogeneous solid occupying domain Ω, see Fig. 2.

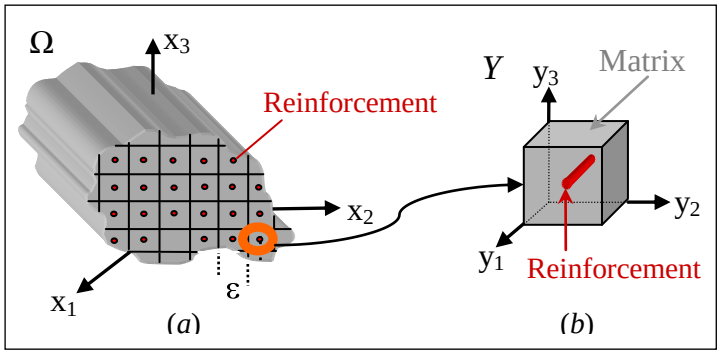

Fig. 2: (a) 3D composite structure, (b) representative unit cell Y.

The elastic deformation of this structure can be described by means of the following boundary-value problem:

$$\sigma^{\varepsilon}_{ij,jx} = f_i \quad \text{in } \Omega \quad \text{and} \quad u^{\varepsilon}_i(\mathbf{x}) = 0 \quad \text{on } \partial\Omega \quad \text{for } i, j = 1, 2, 3 \tag{1}$$

$$\sigma^{\varepsilon}_{ij} = C_{ijkl} e^{\varepsilon}_{kl} \tag{2}$$

$$e^{\varepsilon}_{ij} = 1/2 \; u^{\varepsilon}_{i,jx} + u^{\varepsilon}_{j,ix} \tag{3}$$

In Eqs. (1) and (3) as well as in the rest of the paper we use the following short-hand notation for the derivatives:

$$\phi_{m,nx} = \frac{\partial \phi_m}{\partial x_n} \tag{4}$$

In Eqs. (1) and (3) C_{ijkl} is the tensor of elastic coefficients, e_{kl} is the strain tensor which is a function of the displacement field u_i, and, finally, f_i represent body forces. It is assumed that the C_{ijkl} coefficients are all periodic with a unit cell Y of dimension characterized by a small parameter ε and this small parameter ε is made non-dimensional by dividing the size of the unit cell by a certain characteristic dimension of the overall structure. Consequently, the periodic composite structure in Fig. 2a is seen to be made up of a large number of unit cells periodically arranged within the domain Ω as shown in Fig. 2b.

Asymptotic Expansions, Governing Equations, and Unit Cell Problems

We begin by defining the so-called "fast" or microscopic variables according to:

$$y_i = x_i / \varepsilon \quad , \; i = 1, 2, 3 \tag{5}$$

The boundary value problem and corresponding stress field defined in Eqs. (1) and (2) are transformed into the following expressions:

$$\sigma^{\varepsilon}_{ij,jx} + \varepsilon^{-1}\sigma^{\varepsilon}_{ij,jy} = f_i \quad in\,\Omega \quad \text{and} \quad u^{\varepsilon}_i = 0 \quad on\,\Omega \tag{6}$$

where

$$\sigma^{\varepsilon}_{ij}(\mathbf{x},\mathbf{y}) = C_{ijkl}(\mathbf{y})u_{k,lx}(\mathbf{x},\mathbf{y}) \tag{7}$$

Asymptotic expansions in terms of ε for the displacement and stress fields are next considered:

$$\mathbf{u}^{\varepsilon}(\mathbf{x},\mathbf{y}) = \mathbf{u}^{(0)}(\mathbf{x},\mathbf{y}) + \varepsilon\mathbf{u}^{(1)}(\mathbf{x},\mathbf{y}) + \varepsilon^2\mathbf{u}^{(2)}(\mathbf{x},\mathbf{y}) + \ldots \tag{8}$$

$$\sigma^{\varepsilon}_{ij}(\mathbf{x},\mathbf{y}) = \sigma^{(0)}_{ij}(\mathbf{x},\mathbf{y}) + \varepsilon\sigma^{(1)}_{ij}(\mathbf{x},\mathbf{y}) + \varepsilon^2\sigma^{(2)}_{ij}(\mathbf{x},\mathbf{y}) + \ldots \tag{9}$$

Substitution of Eqs. (8, 9) into Eqs.(1, 2) results, on account of Eq.(3), into the following:

$$\sigma^{(0)}_{ij,jy} = 0 \quad \text{and} \quad \sigma^{(1)}_{ij,jy} + \sigma^{(0)}_{ij,jx} = f_i \tag{10}$$

$$u^{(0)}(\mathbf{x},\mathbf{y}) = u^{(0)}(\mathbf{x}) \quad \text{and} \quad u^{(1)}_m(\mathbf{x},\mathbf{y}) = u^{(0)}_{k,lx}(\mathbf{x})N^{kl}_m(\mathbf{y}) \tag{11}$$

where

$$\sigma^{(0)}_{ij,jy} = C_{ijkl}(u^{(0)}_{k,lx} + u^{(1)}_{k,ly}) \quad \text{and} \quad \sigma^{(1)}_{ij,jy} = C_{ijkl}(u^{(1)}_{k,lx} + u^{(2)}_{k,ly}) \tag{12}$$

and auxiliary functions N^{kl}_m are periodic in y and satisfy

$$\left[C_{ijmn}(\mathbf{y})N^{kl}_{m,ny}(\mathbf{y})\right]_{,jy} = -C_{ijkl,jy}(\mathbf{y}) \tag{13}$$

Eq. (13) is referred to as the *unit-cell problem*. It depends completely on the fast variable ***y***. The next step is the homogenization procedure. This is carried out by substituting (11) into (12), and combining the result with (10). The resulting expression is integrated over the domain Y of the unit cell (with volume $|Y|$) to obtain:

$$\tilde{C}_{ijkl}\frac{\partial^2 u^{(0)}_k}{\partial x_j \partial x_l}\mathbf{x} = f_i \tag{14}$$

where the following definition is introduced:

$$\tilde{C}_{ijkl} = |Y|^{-1}\int_Y C_{ijkl}(\mathbf{y}) + C_{ijmn}(\mathbf{y})N^{kl}_{m,ny}\; dv \tag{15}$$

The coefficients $\tilde{C}_{ijkl}$ denote the homogenized or effective elastic coefficients.

3D GRID-REINFORCED COMPOSITE STRUCTURES

A general 3D orthotropic composite reinforced with ***N*** families of reinforcements will be considered, see Fig. 1. It is assumed that the orthotropic reinforcements have significantly higher elasticity moduli than the matrix material, so we are justified in ignoring the contribution of the matrix phase in the analytical treatment. We first consider a simpler form of unit cell made of only a single reinforcement as shown in Fig. 3a. Having solved this, the effective elastic coefficients of structures with several families of reinforcements can be determined by the superposition of the solution for each of them found separately. One must recognize that an error will be incurred at the regions of intersection between the reinforcements. Nevertheless, our approximation will be quite accurate since these regions of intersection are very much localized and do not add significantly to the integral over the whole unit cell domain. To determine the effective coefficients for the simpler arrangement in Fig. 3a, unit cell problem in Eq. (13) must be solved and (15) must then be applied.

Problem Formulation

We begin with the introduction of the following notation:

$$b_{ij}^{kl} = C_{ijmn}(\mathbf{y}) N_{m,ny}^{kl}(\mathbf{y}) + C_{ijkl} \tag{16}$$

We assume perfect bonding conditions at the interface between the reinforcements and the matrix.

$$N_n^{kl}(r)\Big|_s = N_n^{kl}(m)\Big|_s \quad \text{and} \quad b_{ij}^{kl}(r) n_j\Big|_s = b_{ij}^{kl}(m) n_j\Big|_s \tag{17}$$

Here n_j denote the components of the unit normal vector at the interface and the suffixes *r*, *m*, and *s* refer to the reinforcement, matrix, and reinforcement/matrix interface, respectively.

Since $C_{ijmn}\ m \approx 0$ and hence $b_{ij}^{kl}\ m = 0$, then the interface condition (17) becomes:

$$b_{ij}^{kl}(r) n_j\Big|_s = 0 \tag{18}$$

The unit cell problem that must be solved in combination with Eq. (17) is given by:

$$b_{ij,jy}^{kl} = 0 \tag{19}$$

Coordinate Transformation

To solve the unit cell problem a coordinate transformation of the microscopic coordinate system $\{y_1, y_2, y_3\}$ onto the new coordinate system $\{\eta_1, \eta_2, \eta_3\}$ is performed, see Fig. 3b,

$$\frac{\partial}{\partial y_j} = q_{ij} \frac{\partial}{\partial \eta_i} \tag{20}$$

where q_{ij} are the components of the direction cosines characterizing the axes rotation.

Consequently, the problem at hand becomes independent of η_1 and the solution order is reduced by one.

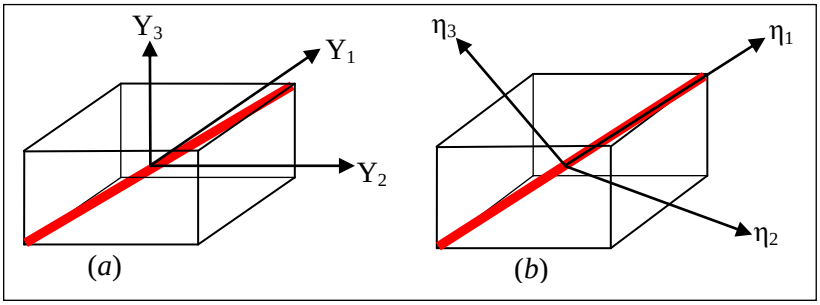

Fig.3 (a) Unit cell in original coordinates, (b) rotated macroscopic coordinates.

Method for Determining Elastic Coefficients

Referring to Fig. 3b, Eqs. (16) and (18) are written in terms of the η_i coordinates to obtain:

$$b_{ij}^{kl} = C_{ijkl}(\mathbf{y}) + C_{ijmn} q_{pn} N_{m,p\eta}^{kl}(\mathbf{y}) \tag{21a}$$

$$b_{ij}^{kl} q_{2j} n_2'(r) + b_{ij}^{kl} q_{3j} n_3'(r) \Big|_s = 0 \tag{21b}$$

Here n_2', n_3' are the components of the unit normal vector in the new coordinate system. Eqs. (21a) and (21b) can be solved by assuming a linear variation of the auxiliary functions N_m^{kl} with respect to η_2 and η_3, i.e.,

$$N_1^{kl} = \lambda_1^{kl}\eta_2 + \lambda_2^{kl}\eta_3, \quad N_2^{kl} = \lambda_3^{kl}\eta_2 + \lambda_4^{kl}\eta_3, \quad N_3^{kl} = \lambda_5^{kl}\eta_2 + \lambda_6^{kl}\eta_3 \tag{22}$$

where λ_i^{kl} are constants to be determined from the boundary conditions. Accordingly, local functions b_{ij}^{kl} in (21a) can be written on the basis of Eq. (22) as follows:

$$b_{mm}^{kl} = C_{mmkl} + \begin{bmatrix} \lambda_1^{kl}\ C_{mm11}q_{21} + C_{mm12}q_{22} + C_{mm13}q_{23} + \lambda_2^{kl}\ C_{mm11}q_{31} + C_{mm12}q_{32} + C_{mm13}q_{33} + \\ +\lambda_3^{kl}\ C_{mm12}q_{21} + C_{mm22}q_{22} + C_{mm23}q_{23} + \lambda_4^{kl}\ C_{mm12}q_{31} + C_{mm22}q_{32} + C_{mm23}q_{33} + \\ +\lambda_5^{kl}\ C_{mm13}q_{21} + C_{mm23}q_{22} + C_{mm33}q_{23} + \lambda_6^{kl}\ C_{mm13}q_{31} + C_{mm23}q_{32} + C_{mm33}q_{33} \end{bmatrix} \tag{23}$$

no summation on m

$$b_{mn}^{kl} = C_{mnkl} + \begin{bmatrix} \lambda_1^{kl}\ C_{mn11}q_{21} + C_{mn12}q_{22} + C_{mn13}q_{23} + \lambda_2^{kl}\ C_{mn11}q_{31} + C_{mn12}q_{32} + C_{mn13}q_{33} + \\ +\lambda_3^{kl}\ C_{mn12}q_{21} + C_{mn22}q_{22} + C_{mn23}q_{23} + \lambda_4^{kl}\ C_{mn12}q_{31} + C_{mn22}q_{32} + C_{mn23}q_{33} + \\ +\lambda_5^{kl}\ C_{mn13}q_{21} + C_{mn23}q_{22} + C_{mn33}q_{23} + \lambda_6^{kl}\ C_{mn13}q_{31} + C_{mn23}q_{32} + C_{mn33}q_{33} \end{bmatrix} \tag{24}$$

with $m \neq n$

The elastic coefficients in Eqs. (23) and (24) are referenced with respect to the $\{y_1, y_2, y_3\}$ coordinate system and are related to the elastic coefficients $C_{rsvw}^{(p)}$ associated with the principal material coordinate system according to:

$$C_{ijkl} = q_{ir} q_{js} q_{kv} q_{lw} C_{rsvw}^{(P)} \tag{25}$$

From Eqs. (21b), (23) and (24) one obtains 6 linear algebraic equations for the solution of λ_i^{kl}. They are:

$$\sum_{m=1}^{6} A_m \lambda_m^{kl} + A_7^{kl} = 0, \sum_{m=8}^{13} A_m \lambda_m^{kl} + A_{14}^{kl} = 0, \sum_{m=15}^{20} A_m \lambda_m^{kl} + A_{21}^{kl} = 0$$
$$\sum_{m=22}^{27} A_m \lambda_m^{kl} + A_{28}^{kl} = 0, \sum_{m=29}^{34} A_m \lambda_m^{kl} + A_{35}^{kl} = 0, \sum_{m=36}^{41} A_m \lambda_m^{kl} + A_{42}^{kl} = 0 \quad (26)$$

Here A_m and A_i^{kl} are constants which depend on the geometric parameters of the unit cell and the material properties of the reinforcement. Once the system of Eq. (26) is solved, the determined λ_i^{kl} coefficients are substituted back into Eqs. (23) and (24) to obtain the local functions b_{ij}^{kl}. In turn, these are used to calculate the effective elastic coefficients of the structure of Fig. 3b. Before closing this Section, it would not be amiss to mention that if we assumed polynomials of a higher order rather than linear variation for N_m^{kl} with respect to η_2 and η_3, then after following the aforementioned procedure and comparing terms of equal powers of η_2 and η_3, all of the terms would vanish except the linear ones.

Effective Elastic Coefficients

The effective elastic coefficients for the 3D grid-reinforced composite with generally orthotropic reinforcements are obtained from Eqs. (15) and (16):

$$\tilde{C}_{ijkl} = (AL/V) b_{ij}^{kl} = V_f b_{ij}^{kl} \quad (27)$$

Here b_{ij}^{kl} are elastic constants, L and A are, repectively, the length and cross-sectional area of the reinforcement (in coordinates y_1, y_2, y_3), V is the volume of the unit cell and V_f is the volume fraction of the reinforcement within the unit cell. It can be proved that the effective elastic coefficients maintain the same symmetry and convexity properites as their actual material counterparts, see, e.g., Bakhvalov and Panasenko [11]. Expression (27) pertains to grid-reinforced structures with a single family of reinforcements. For structures with more than one family of reinforcements the effective moduli can be found by superposition. Thus, the effective elastic coefficients of a grid-reinforced structure with $\boldsymbol{N}$ families of reinforcements are,

$$\tilde{C}_{ijkl} = \sum_{n=1}^{N} V_f^{(n)} b_{ij}^{(n)kl} \quad (28)$$

where the superscript (n) represents the *n-th* reinforcement family.

EXAMPLES OF GRID-REINFORCED STRUCTURES

The developed micromechanical model is used to study different examples of grid-reinforced composite structures with orthotropic reinforcements.

Example 1: Cubic Grid-Reinforced Composite with Orthotropic Reinforcement

This example pertains to the cubic grid-reinforced structure shown in Fig. 1. This structure has three families of generally orthotropic reinforcements, each family oriented along one of the coordinate axes. Following the determination of the local functions b_{ij}^{kl} from Eqs. (23) and (24), the non-vanishing elastic effective coefficients for the composite grid-structure are given by:

$$\tilde{C}_{11} = (A_1 L_1 / V) E_1^{\,j} \; ; \quad \tilde{C}_{22} = (A_2 L_2 / V) E_1^{\,j} \; ; \quad \tilde{C}_{33} = (A_3 L_3 / V) E_1^{\,j} \tag{29}$$

Here, $E_1^{\,j}$ is the principal Young's modulus of the reinforcement oriented in the y_j direction.

Example 2: 2D Grid-Reinforced Composite

This example validates the convergence of model for the case of 2D grid-reinforced structures whereby reinforcements are isotropic and lie entirely in the $y_1 - y_2$ plane. We first solve for λ_i^{kl} from Eq. (26) and then obtain the local functions b_{ij}^{kl} from Eqs. (23) and (24). Following that, the effective elastic coefficients (in terms of Young's modulus of the reinforcement, E) are given by:

$$\begin{aligned} &\tilde{C}_{11} = (AL/V)E\cos^4\theta; \quad \tilde{C}_{22} = (AL/V)E\sin^4\theta; \quad \tilde{C}_{12} = \tilde{C}_{66} = (AL/V)E\cos^2\theta \sin^2\theta \\ &\tilde{C}_{16} = (AL/V)E\cos^3\theta \sin\theta; \quad \tilde{C}_{26} = (AL/V)E\cos\theta \sin^3\theta; \quad \tilde{C}_{ij} = \tilde{C}_{ji} \end{aligned} \tag{30}$$

These results are the same those obtained earlier by Kalamkarov [4], who used asymptotic homogenization techniques, and by Pshenichnov [12], who used a different approach based on stress-strain relationships in the reinforcements.

Example 3: Conical Arrangement of Generally Orthotropic Reinforcements

The unit cell of this structure, S_1, is shown in Fig. 4a. Although, the expressions for the effective elastic coefficients are too lengthy to be reproduced here, some of these coefficients will be plotted vs. V_f or vs. the inclination of the reinforcements with the y_3.

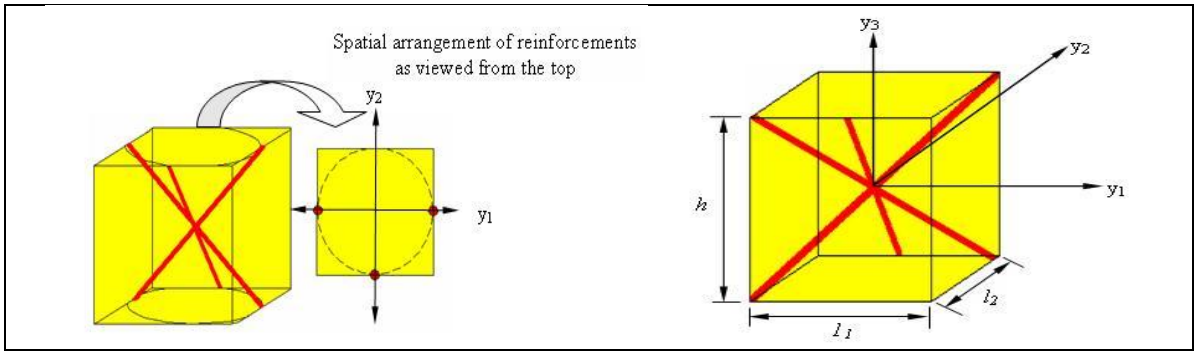

Fig. 4a: Conically reinforced structure, S_1. Fig. 4b: Diagonally reinforced structure, S_2.

Example 4: Diagonally Oriented Generally Orthotropic Reinforcements

The general unit cell of this example, S_2, is formed by orienting three reinforcements as shown in Fig. 4b. The effective elastic coefficients can be calculated following the same approach as that used in the previous examples. The resulting expressions for some of the effective coefficients will be represented graphically in the next section.

NUMERICAL RESULTS AND DISCUSSION

The mathematical model and methodology presented can be used in analysis and design to tailor the effective elastic coefficients of any 3D composite grid structure by varying the

material, number, orientation and cross-sectional area of the reinforcements. In this Section typical effective elastic coefficients will be computed and plotted. The reinforcements have material properties given in Table 1 [10].

Table 1: Properties of Reinforcement Material [10]

Elastic Properties								
E_1 (MPa)	E_2 (MPa)	E_3 (MPa)	G_{12} (MPa)	G_{13} (MPa)	G_{23} (MPa)	ν_{12}	ν_{13}	ν_{23}
173058	33065	5171	9377	8274	3240	0.036	0.25	0.171

Typical effective coefficients of structure S_1 are plotted vs. the angle of inclination of the reinforcements to the y_3 axis. As this angle increases, the reinforcements are oriented progressively closer to in the y_1–y_2 plane, and, consequently, further away from the y_3 axis. Thus, one anticipates a corresponding increase in the value of $\tilde{C}_{22}$ and a decrease in the value of $\tilde{C}_{33}$. Fig. 5 illustrates precisely this point.

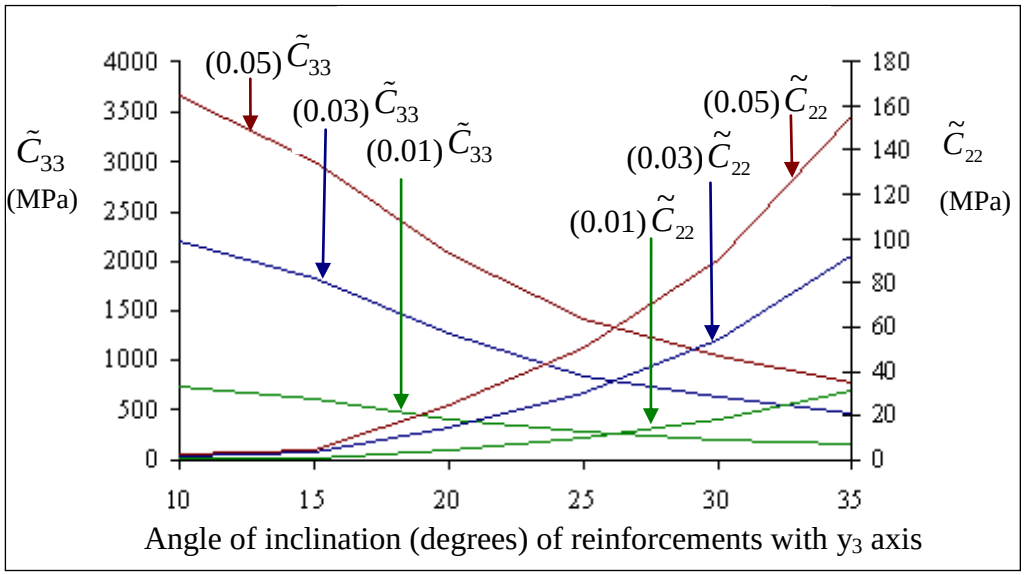

Fig. 5: $\tilde{C}_{22}$, $\tilde{C}_{33}$ vs. volume fractions/inclination of reinforcements with the y_3 for S_1

We next plot some of the effective coefficients vs. the relative height of the unit cell for structure S_2 shown in Fig. 4b. The relative height is defined as the ratio of the height to the length of the unit cell. Increasing the relative height will decrease the volume fraction of the reinforcements and at the same time will decrease the orientation angle between the reinforcements and the y_3 axis. Both of these factors tend to reduce the stiffnesses in the y_1 and y_2 directions. Fig. 6 demonstrates this point for the cases of $\tilde{C}_{11}, \tilde{C}_{22}, \tilde{C}_{66}$. The stiffness in y_3 direction however increases. This is because the decrease in the angle of inclination of the reinforcements to the y_3 axis (which increases the value of $\tilde{C}_{33}$) dominates the decrease in the volume fraction.

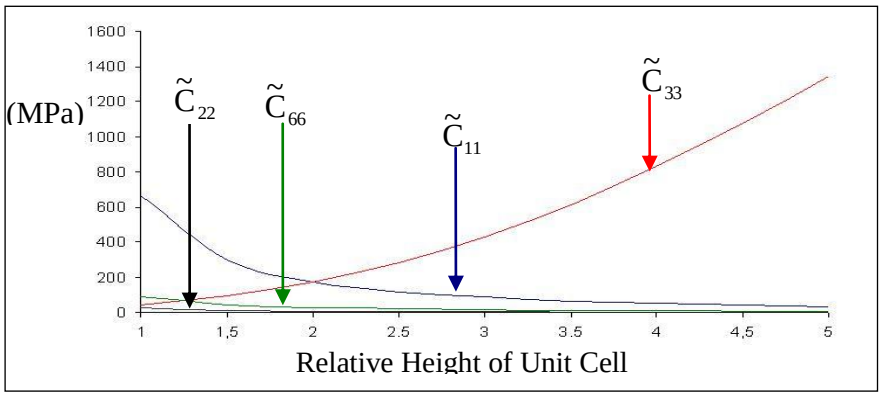

Fig. 6: $\tilde{C}_{11}$, $\tilde{C}_{22}$, $\tilde{C}_{33}$, and $\tilde{C}_{66}$ effective coefficient vs. relative height of the unit cell for S_2.

We will also compare a typical effective coefficient of structures S_1 and S_2 by varying the overall volume fraction of the reinforcements. For S_1 we do so by varying the cross-sectional area of the reinforcements and for S_2 we do so by changing the relative height of the unit cell. The results are shown in Fig. 7. The general trends depicted in the plot are logical on account of the different ways in which the volume fraction is varied. For S_1 we increase the volume fraction by increasing the cross-sectional area of the reinforcements and hence we predict a corresponding increase in $\tilde{C}_{33}$. Pertinent to S_2 however, by decreasing the relative height of the unit cell (in order to increase the overall reinforcement volume ratio) we, at the same time, increase the angle of inclination of the reinforcements with y_3. Since the reinforcements are now oriented further away from the y_3 the value of $\tilde{C}_{33}$ is expected to decrease. Furthermore, this decrease dominates the increase in the stiffness value due to the volume fraction increasing. Hence, the net effect is an overall decrease in $\tilde{C}_{33}$ *albeit* in a non-linear mode. Thus, it is seen that beyond a certain volume fraction, S_1 is stiffer than S_2 under these circumstances. This trend can of course be easily changed. For example, had we increased the volume fraction of S_2 by simply changing the cross-sectional area of the reinforcements and leaving the relative height of the unit cell the same, then a higher volume fraction would naturally translate into larger $\tilde{C}_{33}$ values.

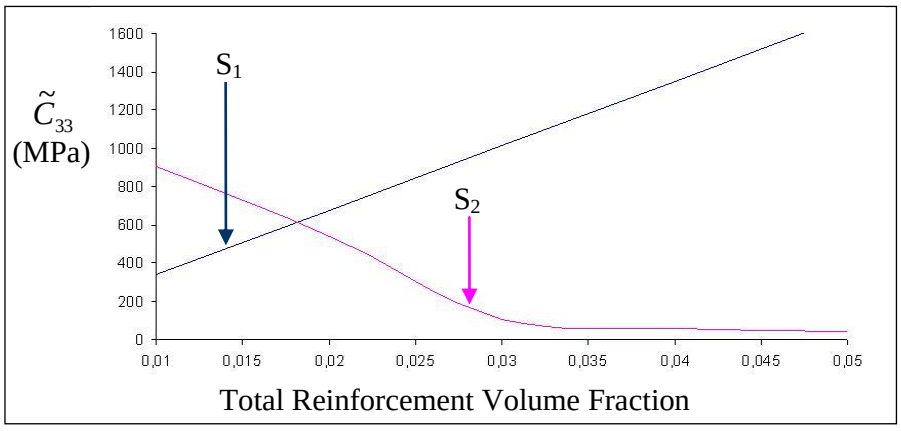

Fig. 7: Plot of $\tilde{C}_{33}$ vs. total volume fraction for structures S_1 (Fig. 4a) and S_2 (Fig. 4b).

CONCLUSIONS

The asymptotic homogenization method is used to develop a comprehensive 3D micromechanical model pertaining to globally anisotropic periodic composite structures reinforced with an embedded grid of generally orthotropic reinforcements. The general orthotropy of the material of reinforcements which is very significant from practical point of view renders the problem much more complex. The model developed transforms the original boundary-value problem into a much simpler one characterized by the effective elastic coefficients. These effective coefficients are shown to depend only on the geometric and material parameters of the unit cell and are free from the inhomogeneity complications that characterize their original material counterparts. As a consequence, they can be used to study a wide variety of boundary value problems associated with the composite of a given microstructure. The developed model is applied to different examples of orthotropic composite structures.

ACKNOWLEDGEMENT

This work has been supported by the Natural Sciences and Engineering Research Council of Canada (NSERC).

REFERENCES

1. Bensoussan A, Lions JL, Papanicolaou G. Asymptotic analysis for periodic structures, Amsterdam: North-Holland Publishing Company; 1978.
2. Duvaut G. Analyse fonctionnelle et méchanique des milieux continues. In: Proceeding of the 14th IUTAM Congress, Delft, The Netherlands, 1976. p. 119-32.
3. Caillerie D. Thin elastic and periodic plates. Math Appl Sci, 1984;6:159–91.
4. Kalamkarov AL. Composite and Reinforced Elements of Construction. Chichester, New York: Wiley; 1992.
5. Kalamkarov AL, Kolpakov AG. A new asymptotic model for a composite piezoelastic plate. Int J Solids Struct 2001;38:6027–44.
6. Kalamkarov AL, Georgiades AV. Modeling of Smart Composites on Account of Actuation, Thermal Conductivity and Hygroscopic Absorption. Composites part B: Eng 2002a;33:141–52.
7. Kalamkarov AL, Georgiades A.V. Micromechanical Modeling of Smart Composite Structures. Smart Materials Struct 2002b;11:423–34.
8. Georgiades AV, Challagulla KS, Kalamkarov AL. Modeling of the thermopiezoelastic behavior of prismatic smart composite structures made of orthotropic materials. Composites part B: Eng 2006;37:569–582.
9. Challagulla KS, Georgiades AV, Kalamkarov AL. Asymptotic homogenization modeling of thin network structures. Compos Struct 2007;(3):432–44.
10. Reddy JN. Mechanics of Laminated Composite Plates. New York: CRC Press; 1997.
11. Bakhvalov N, Panasenko G. Homogenization: Averaging processes in periodic media. Netherland: Kluwer Academic.Publisher; 1984.
12. Pshenichnov GI. Theory of Thin Elastic Network Plates and Shells. Moscow: Nauka; 1982.